

# World Journal of *Gastroenterology*

*World J Gastroenterol* 2021 September 14; 27(34): 5625-5795



**EDITORIAL**

- 5625 Serrated lesions: A challenging enemy  
*Trovato A, Turshudzhyan A, Tadros M*

**REVIEW**

- 5630 Liver disorders in COVID-19, nutritional approaches and the use of phytochemicals  
*Vargas-Mendoza N, García-Machorro J, Angeles-Valencia M, Martínez-Archundia M, Madrigal-Santillán EO, Morales-González Á, Anguiano-Robledo L, Morales-González JA*
- 5666 Recent advances in blood-based and artificial intelligence-enhanced approaches for gastrointestinal cancer diagnosis  
*Li LS, Guo XY, Sun K*
- 5682 Liver disease and COVID-19: The link with oxidative stress, antioxidants and nutrition  
*Ristic-Medic D, Petrovic S, Arsic A, Vucic V*

**MINIREVIEWS**

- 5700 Updates in diagnosis and management of pancreatic cysts  
*Lee LS*
- 5715 Artificial intelligence for hepatitis evaluation  
*Liu W, Liu X, Peng M, Chen GQ, Liu PH, Cui XW, Jiang F, Dietrich CF*
- 5727 Machine perfusion of the liver: Putting the puzzle pieces together  
*Boteon YL, Martins PN, Muiesan P, Schlegel A*

**ORIGINAL ARTICLE****Retrospective Cohort Study**

- 5737 *MTNR1B* polymorphisms with *CDKN2A* and *MGMT* methylation status are associated with poor prognosis of colorectal cancer in Taiwan  
*Lee CC, Kuo YC, Hu JM, Chang PK, Sun CA, Yang T, Li CW, Chen CY, Lin FH, Hsu CH, Chou YC*

**Retrospective Study**

- 5753 Validation of conventional non-invasive fibrosis scoring systems in patients with metabolic associated fatty liver disease  
*Wu YL, Kumar R, Wang MF, Singh M, Huang JF, Zhu YY, Lin S*

**Observational Study**

- 5764 Secular decreasing trends in gastric cancer incidence in Taiwan: A population-based cancer registry study  
*Lin YT, Chiang CJ, Yang YW, Huang SP, You SL*

**META-ANALYSIS**

- 5775** Dietary intake in patients with chronic pancreatitis: A systematic review and meta-analysis  
*Ul Ain Q, Bashir Y, Kelleher L, Bourne DM, Egan SM, McMahon J, Keaskin L, Griffin OM, Conlon KC, Duggan SN*

**LETTER TO THE EDITOR**

- 5793** Relationship between nonalcoholic fatty liver disease and chronic kidney disease could start in childhood  
*Di Sessa A, Guarino S, Melone R, De Simone RF, Marzuillo P, Miraglia del Giudice E*

**ABOUT COVER**

Editorial Board Member of *World Journal of Gastroenterology*, Konstantinos Triantafyllou, MD, PhD, FEBGH, Professor, Hepatogastroenterology Unit, 2nd Department of Propaedeutic Internal Medicine, Medical School, National and Kapodistrian University of Athens, Attikon University General Hospital, 1, Rimini Street, Athens 12462, Greece. ktriant@med.uoa.gr

**AIMS AND SCOPE**

The primary aim of *World Journal of Gastroenterology* (*WJG, World J Gastroenterol*) is to provide scholars and readers from various fields of gastroenterology and hepatology with a platform to publish high-quality basic and clinical research articles and communicate their research findings online. *WJG* mainly publishes articles reporting research results and findings obtained in the field of gastroenterology and hepatology and covering a wide range of topics including gastroenterology, hepatology, gastrointestinal endoscopy, gastrointestinal surgery, gastrointestinal oncology, and pediatric gastroenterology.

**INDEXING/ABSTRACTING**

The *WJG* is now indexed in Current Contents®/Clinical Medicine, Science Citation Index Expanded (also known as SciSearch®), Journal Citation Reports®, Index Medicus, MEDLINE, PubMed, PubMed Central, and Scopus. The 2021 edition of Journal Citation Report® cites the 2020 impact factor (IF) for *WJG* as 5.742; Journal Citation Indicator: 0.79; IF without journal self cites: 5.590; 5-year IF: 5.044; Ranking: 28 among 92 journals in gastroenterology and hepatology; and Quartile category: Q2. The *WJG*'s CiteScore for 2020 is 6.9 and Scopus CiteScore rank 2020: Gastroenterology is 19/136.

**RESPONSIBLE EDITORS FOR THIS ISSUE**

Production Editor: Ji-Hong Lin; Production Department Director: Yu-Jie Ma; Editorial Office Director: Ze-Mao Gong.

**NAME OF JOURNAL**

*World Journal of Gastroenterology*

**ISSN**

ISSN 1007-9327 (print) ISSN 2219-2840 (online)

**LAUNCH DATE**

October 1, 1995

**FREQUENCY**

Weekly

**EDITORS-IN-CHIEF**

Andrzej S Tarnawski, Subrata Ghosh

**EDITORIAL BOARD MEMBERS**

<http://www.wjgnet.com/1007-9327/editorialboard.htm>

**PUBLICATION DATE**

September 14, 2021

**COPYRIGHT**

© 2021 Baishideng Publishing Group Inc

**INSTRUCTIONS TO AUTHORS**

<https://www.wjgnet.com/bpg/gerinfo/204>

**GUIDELINES FOR ETHICS DOCUMENTS**

<https://www.wjgnet.com/bpg/GerInfo/287>

**GUIDELINES FOR NON-NATIVE SPEAKERS OF ENGLISH**

<https://www.wjgnet.com/bpg/gerinfo/240>

**PUBLICATION ETHICS**

<https://www.wjgnet.com/bpg/GerInfo/288>

**PUBLICATION MISCONDUCT**

<https://www.wjgnet.com/bpg/gerinfo/208>

**ARTICLE PROCESSING CHARGE**

<https://www.wjgnet.com/bpg/gerinfo/242>

**STEPS FOR SUBMITTING MANUSCRIPTS**

<https://www.wjgnet.com/bpg/GerInfo/239>

**ONLINE SUBMISSION**

<https://www.f6publishing.com>

## Artificial intelligence for hepatitis evaluation

Wei Liu, Xue Liu, Mei Peng, Gong-Quan Chen, Peng-Hua Liu, Xin-Wu Cui, Fan Jiang, Christoph F Dietrich

**ORCID number:** Wei Liu 0000-0001-7777-5507; Xue Liu 0000-0003-4148-6812; Mei Peng 0000-0001-7809-9440; Gong-Quan Chen 0000-0002-4204-6133; Peng-Hua Liu 0000-0003-1981-7451; Xin-Wu Cui 0000-0003-3890-6660; Fan Jiang 0000-0001-8896-2009; Christoph F Dietrich 0000-0001-6015-6347.

**Author contributions:** Cui XW, Jiang F, and Dietrich CF established the design and conception of the paper; Liu W, Liu X, Peng M, Chen GQ, Liu PH, Jiang F, Cui XW, and Dietrich CF explored the literature data; Liu W provided the first draft of the manuscript, which was discussed and revised critically for intellectual content by Liu X, Peng M, Chen GQ, Liu PH, Jiang F, Cui XW, and Dietrich CF; all authors discussed the statement and conclusions and approved the final version to be published.

**Supported by** the National Natural Science Foundation of China, No. 82071953; and Department of Science and Technology of Hunan Province, No. 2020SK52103.

**Conflict-of-interest statement:**

There is no conflict of interest associated with any of the senior author or other coauthors who contributed their efforts in this manuscript.

**Open-Access:** This article is an open-access article that was

**Wei Liu, Xue Liu, Mei Peng, Fan Jiang,** Department of Medical Ultrasound, The Second Hospital of Anhui Medical University, Hefei 230601, Anhui Province, China

**Gong-Quan Chen,** Department of Medical Ultrasound, Minda Hospital of Hubei Minzu University, Enshi 445000, Hubei Province, China

**Peng-Hua Liu,** Department of Medical Ultrasound, The First Affiliated Hospital of Shaoyang University, Shaoyang 422000, Hunan Province, China

**Xin-Wu Cui,** Sino-German Tongji-Caritas Research Center of Ultrasound in Medicine, Department of Medical Ultrasound, Tongji Hospital, Tongji Medical College, Huazhong University of Science and Technology, Wuhan 430030, Hubei Province, China

**Christoph F Dietrich,** Department Allgemeine Innere Medizin, Kliniken Hirslanden Beau Site, Salem und Permanence, Bern 3626, Switzerland

**Corresponding author:** Xin-Wu Cui, MD, PhD, Professor, Sino-German Tongji-Caritas Research Center of Ultrasound in Medicine, Department of Medical Ultrasound, Tongji Hospital, Tongji Medical College, Huazhong University of Science and Technology, No. 1095 Jiefang Avenue, Wuhan 430030, Hubei Province, China. [cuixinwu@live.cn](mailto:cuixinwu@live.cn)

### Abstract

Recently, increasing attention has been paid to the application of artificial intelligence (AI) to the diagnosis of diverse hepatic diseases, which comprises traditional machine learning and deep learning. Recent studies have shown the possible value of AI based data mining in predicting the incidence of hepatitis, classifying the different stages of hepatitis, diagnosing or screening for hepatitis, forecasting the progression of hepatitis, and predicting response to antiviral drugs in chronic hepatitis C patients. More importantly, AI based on radiology has been proven to be useful in predicting hepatitis and liver fibrosis as well as grading hepatocellular carcinoma (HCC) and differentiating it from benign liver tumors. It can predict the risk of vascular invasion of HCC, the risk of hepatic encephalopathy secondary to hepatitis B related cirrhosis, and the risk of liver failure after hepatectomy in HCC patients. In this review, we summarize the application of AI in hepatitis, and identify the challenges and future perspectives.

**Key Words:** Machine learning; Deep learning; Radiomics; Hepatitis; Fibrosis; Hepatocellular carcinoma

©The Author(s) 2021. Published by Baishideng Publishing Group Inc. All rights reserved.

selected by an in-house editor and fully peer-reviewed by external reviewers. It is distributed in accordance with the Creative Commons Attribution NonCommercial (CC BY-NC 4.0) license, which permits others to distribute, remix, adapt, build upon this work non-commercially, and license their derivative works on different terms, provided the original work is properly cited and the use is non-commercial. See: <http://creativecommons.org/licenses/by-nc/4.0/>

**Manuscript source:** Invited manuscript

**Specialty type:** Gastroenterology and hepatology

**Country/Territory of origin:** China

**Peer-review report's scientific quality classification**

Grade A (Excellent): 0  
Grade B (Very good): 0  
Grade C (Good): C, C  
Grade D (Fair): 0  
Grade E (Poor): 0

**Received:** March 1, 2021

**Peer-review started:** March 1, 2021

**First decision:** April 18, 2021

**Revised:** April 28, 2021

**Accepted:** August 2, 2021

**Article in press:** August 2, 2021

**Published online:** September 14, 2021

**P-Reviewer:** Borzi L

**S-Editor:** Zhang H

**L-Editor:** Wang TQ

**P-Editor:** Liu JH



**Core Tip:** Currently, there is a need of a comprehensive review to introduce the applications of artificial intelligence (AI) in hepatitis. We first discuss the possible value of AI based data mining in predicting the incidence of hepatitis, classifying the different stages of hepatitis, diagnosing or screening for hepatitis, forecasting the progression of hepatitis, and predicting response to antiviral drugs in chronic hepatitis C patients. In addition, we introduce the applications of AI based on radiology in predicting hepatitis and liver fibrosis, grading hepatocellular carcinoma (HCC) and differentiating it from benign liver tumors, and predicting the risk of vascular invasion of HCC as well as the risk of hepatic encephalopathy secondary to hepatitis B related cirrhosis.

**Citation:** Liu W, Liu X, Peng M, Chen GQ, Liu PH, Cui XW, Jiang F, Dietrich CF. Artificial intelligence for hepatitis evaluation. *World J Gastroenterol* 2021; 27(34): 5715-5726

**URL:** <https://www.wjgnet.com/1007-9327/full/v27/i34/5715.htm>

**DOI:** <https://dx.doi.org/10.3748/wjg.v27.i34.5715>

## INTRODUCTION

Artificial intelligence (AI) is a new discipline that aims to simulate, extend, and expand human intelligence and integrates theory, method, and application research and development[1]. According to the different algorithms of AI, AI is usually divided into traditional AI (*e.g.*, traditional machine learning) and deep learning (based on neural network structure) in the medical field[2]. Compared with traditional AI, deep learning can directly apply the image to the learning process without manual feature extraction, while traditional machine learning needs manual recognition and extraction of different features. Therefore, deep learning has the advantage of no manual extraction of various features, which makes its learning process faster, intelligent, and accurate. In addition, deep learning can iterate and improve from past mistakes, but it needs more big data and more result analysis to fully show its robust and precise efficiency[3].

Lately, AI technology has been at the forefront of scientific research. The benefits of the AI model in various fields have triggered an upsurge in the use of this technology for data mining and analysis in more areas, and it has also attracted attention in the field of medicine and biological cognition[4]. For instance, AI has been widely used in the examination of superficial glands such as the thyroid and breast to assist radiologists to evaluate whether nodules are benign or malignant, with a high level of accuracy. The accuracy is lower than that of senior radiologists but higher than that of junior radiologists[5-7]. Some literature has reported the application of AI technology based on data mining or radiology in predicting hepatitis, evaluating fibrosis, and diagnosing benign and malignant liver masses[8-10].

This systematic review is intended to ascertain the clinical utility in routine practice of AI based on data mining, predict the incidence of hepatitis A, B, C, or E, categorize the different stages of hepatitis B, predict the progression of hepatitis C in veterans, and diagnose or screen for hepatitis B. Particularly, this review focuses on the application of deep learning or radiomics based on radiology to stage hepatic fibrosis, predict the occurrence of HCC, identify microvascular invasion, and predict the risk of liver failure after hepatectomy in HCC patients.

## HEPATITIS DETECTION BASED ON DATA MINING

### *Predicting incidence of hepatitis*

Newborn babies are required to be vaccinated with hepatitis B vaccine in numerous countries, which has reduced the incidence of hepatitis worldwide. However, viral hepatitis is still a serious health problem[11]. Hence, Guan *et al*[12] designed the AI model of artificial neural network (ANN) and autoregressive integrated moving average (ARIMA) with hepatitis data mined from Liaoning Disease Control and Prevention Center, which aimed to forecast the incidence of hepatitis A. They extracted data concerning the incidence of hepatitis A from 1987 to 2001 in the above-mentioned Disease Control and Prevention Center. The incidence of hepatitis A from

1981 to 1997 was taken as the training group and from 1998 to 2001 as the validation group. The forecasting statistical effect value and the correlation coefficient are summarized in [Table 1](#). Intelligently mining hepatitis B-related medical record data from local health websites authorized by the local Health Commission, the AI model of ARIMA (0, 1, 1) and ElmanNN (Elman neural network) with eight neurons were established by Zheng *et al*[13]. From January 2012 to August 2019, the local health bureau reported 486983 cases of hepatitis B. Hepatitis B incidence from January 2012 to December 2018 was used to build and train ARIMA (0, 1, 1) model and ElmanNN model with eight neurons, and hepatitis B incidence from January 2019 to August 2019 was used to validate ARIMA (0, 1, 1) model and ElmanNN with eight neurons, with root-mean-square error (RMSE) and mean absolute error (MAE) applied to evaluate the prediction effect of the model. The RMSE and MAE of the above-mentioned ARIMA (0, 1, 1) model and ElmanNN with eight neurons are shown in [Table 1](#). Gan *et al*[14] also tried to forecast the incidence of hepatitis B using a hybrid model combining Grey system and BP-ANN (back propagation artificial neural networks), with trained and validated data collected from National Health Commission. From 2003 to 2012, 10486959 cases of hepatitis B were reported by National Health Commission. Compared with the above data, the prediction effect of a hybrid model, Grey model (1, 1) and Grey model (2, 1), was calculated. The predictive results are summarized in [Table 1](#). The results showed that the hybrid algorithm was superior to the Grey model algorithm in all assessment norms, and a better prediction effect was achieved. Intending to predict the incidence of hepatitis E, Guo *et al*[15] mined monthly incidence and cases of hepatitis E from the local Center for Disease Control and Prevention as samples. All above-mentioned data were collected from January 2005 to December 2017 in the local Centers for Disease Control. The monthly incidence and cases from January 2005 to June 2015 were used as the input variable to establish an AI model of the ARIMA, supporter vector machine (SVM), and long-short time memory neural network (LSTM), and those from July 2015 to December 2017 as the validating group. The assessment indexes of the ARIMA, SVM, and LSTM models were RMSE and MAE, whose corresponding values are given in [Table 1](#).

### **Classifying different stages of hepatitis**

According to the serological level of transaminase and serological titer of hepatitis B antigen or antibody, hepatitis B can be categorized into five stages: I, HBeAg (+) chronic infection; II, HBeAg (+) chronic hepatitis; III, HBeAg (-) chronic infection; IV, HBeAg (-) chronic hepatitis; V, HBsAg (-) stage. For young doctors, it can be difficult to accurately classify the clinical types of hepatitis. Therefore, with 52 patients included, an automated diagnosis of hepatitis B using multilayer mamdani fuzzy inference system expert system (ADHB-ML-MFIS) was established by Ahmad *et al*[16] to categorize the different stages of hepatitis B. In the ADHB-ML-MFIS expert system, there were two levels of input variables. The input variables of the first layer were transaminase, and the input variables of the second layer were serological markers of hepatitis B. The diagnostic accuracy of the ADHB-ML-MFIS expert system for differentiating stages of hepatitis B was 92.2% with the detailed results shown in [Table 1](#).

### **Diagnosing or screening for hepatitis**

Raman spectroscopy has been used to diagnose hepatitis B, showing a superior performance compared to traditional serological tests. Obtaining 119 confirmed hepatitis B virus (HBV) infected samples from histopathology department, Khan *et al* [8] combined Raman spectroscopy with pattern recognition technology, and established an AI model based on the SVM algorithm and radial basis function to diagnose hepatitis B. In the study, the AI model achieved high diagnostic performance for hepatitis B, with the data presented in [Table 1](#). Collecting data from 1134 blood samples, Wang *et al*[17] proposed a method for promptly screening hepatitis B patients and non-hepatitis B patients using serum Raman spectroscopy combined with LSTM. Then, LSTM was used to train the spectral data. Several models can distinguish hepatitis B from non-hepatitis B, with the highest diagnostic efficacy acquired by serum Raman spectroscopy combined with LSTM. The accuracy of serum Raman spectroscopy combined with LSTM for screening hepatitis B from non-hepatitis B was 0.9732. About 50% of hepatitis C virus (HCV) infected persons worldwide have not been diagnosed or treated, and it remains a significant risk factor for human health [18]. Thus, it is vital that clinicians could find these undiagnosed patients with hepatitis C infection, a nowadays-treatable disease. With 120023 HCV patients and 9601900 non-HCV patients used as modeling data, Doyle *et al*[19] developed five kinds of AI models attempting to find undiagnosed hepatitis C infection: Logistic regression, gradient boosting trees, gradient boosting trees with temporal variables, stacked

**Table 1** Hepatitis detection based on data mining

No.	Task	Algorithms	Sample size (type)	Evaluation index	Ref.
1	Predicting incidence of hepatitis A	ANN; ARIMA	N/A (CDC data)	ANN: Correlation coefficient 0.71; ARIMA: Correlation coefficient 0.66	[12]
2	Predicting incidence of hepatitis B	ARIMA; ElmanNN	486983 cases (data from health commission)	ARIMA: RMSE 0.94, MAE 0.81; ElmanNN: RMSE 0.89, MAE 0.70	[13]
3	Forecasting incidence of hepatitis B	Hybrid method (combing GM and BP-ANN)	10486959 cases (data from health ministry)	R 0.9495, RMSE $4.863 \times 10^3$ , MAE $3.9704 \times 10^4$	[14]
4	Prediction of incidence of hepatitis E	ARIMA; SVM; LSTM	N/A (CDC data)	ARIMA: RMSE 0.022, MAE 0.018; SVM: RMSE 0.0204, MAE 0.0167; LSTM: RMSE 0.01, MAE 0.011	[15]
5	Automated classification of the different stages of hepatitis B	ADHB-ML-MFIS expert system	52 patients (serological data)	Overall accuracy: 0.922; No hepatitis accuracy: 1; Due to infection accuracy: 0.75; Acute HBV accuracy: 0.95; Chronic HBV accuracy: 0.91	[16]
6	Analyzing HBV infection from normal blood samples	Polynomial function; RBF	119 serum samples from HBV infected patients (Raman spectroscopy data)	Polynomial kernel (order-2): Quadratic programming/least squares: Accuracy 98%, precision 97%, sensitivity 100%, specificity 95%; RBF kernel (RBF sigma-2): Quadratic programming: accuracy 94%, precision 90%, sensitivity 100%, specificity 87%; RBF kernel (RBF sigma-2): Least squares: Accuracy 95%, precision 92%, sensitivity 100%, specificity 90%	[8]
7	Rapidly screening hepatitis B from non-hepatitis B	LSTM	1134 blood samples (Raman spectroscopy data)	Accuracy 97.32%, sensitivity 97.87%, specificity 96.77%, precision 96.84%	[17]
8	Finding undiagnosed patients with hepatitis C infection	Logistic regression; Gradient boosting trees; Gradient boosting trees with temporal variables; Stacked ensemble; Random forest	9721923 patients (data from the patient's medical history)	The stacked ensemble had a specificity of 0.99 and precision of 0.97 at a recall level of 0.50	[19]
9	Predicting hepatitis C virus progression among veterans	CS Cox model; longitudinal Cox model; CS boosting model; Longitudinal-boosting model	72683 CHC individuals (VHA data)	CS Cox model: Concordance 0.746; Longitudinal Cox model: Concordance 0.764; CS boosting model: Concordance 0.758; Longitudinal-boosting model: Concordance 0.774	[20]
10	Forecasting response to IFN plus RIB treatment in HCV patients	ANN	300 patients (serological data)	The diagnostic accuracy rose from 52% (ANN 2) to 70% (ANN 6)	[21]

ANN: Artificial neural network; ARIMA: Autoregressive integrated moving average; CDC: Centers for Disease Control; RMSE: Root-mean-square error; MAE: Mean absolute error; GM: Grey model, BP-ANN: Back propagation artificial neural networks; SVM: Supporter vector machine; LSTM: Long-short time memory neural network; ADHB-ML-MFIS: Automated diagnosis of hepatitis B using multilayer Mamdani fuzzy inference; HBV: Hepatitis B virus; RBF: Gaussian radial basic function; CHC: Chronic hepatitis C virus; VHA: National Veterans Health Administration; IFN: Interferon; RIB: Ribavirin, HCV: Hepatitis C virus.

ensemble, and random forest. All these models mined data from demographics, risk factors, symptoms, treatments, and procedures relevant to HCV from the patient's medical history. At different recall levels, the models had different diagnostic performances. For example, the stacked ensemble had a specificity of 0.99 and precision of 0.97 at a recall level of 0.50.

### Forecasting progression of hepatitis

Liver biopsy is the gold standard for the evaluation of liver fibrosis and cirrhosis. However, liver biopsy is an invasive examination and carries the risk of causing liver bleeding. In clinical practice, aspartate aminotransferase-to-platelet ratio index (APRI) and radiology are often used to forecast hepatic fibrosis and cirrhosis. In Konerman *et al*[20]'s study, aiming to predict HCV progression among veterans, they developed the cross-sectional (CS) Cox model, longitudinal Cox model, CS boosting model, and longitudinal-boosting model with 72683 chronic hepatitis C (CHC) individuals and matched control data searched from National Veterans Health Administration between 2000 and 2016. The calculated value of APRI > 2 after time zero for two consecutive times indicated the progression of liver cirrhosis. The predictive

concordance of the above-mentioned four models is given in [Table 1](#).

### **Predicting response to antiviral drugs in CHC patients**

The combined administration of interferon-alpha (IFN) and ribavirin (RIB) is the first-line recommended treatment regimen for patients with CHC. However, the cure rate is still low and the incidence of side effects is high. Therefore, there is an urgent need for doctors in the hepatology or infection departments to evaluate the response of patients with CHC to the combinative administration of IFN and RIB. Hence, Maiellaro *et al*[21] retrospectively analyzed 300 patients treated with IFN plus RIB through an ANN, intending to predict the response to the treatment. The range of positive predictive value and negative predictive value of the ANN model for predicting the treatment response of patients with CHC to the combined administration of IFN and RIB was 57%-75% and 52%-71%, respectively.

## **HEPATITIS EVALUATION BASED ON RADIOLOGY**

Radiology plays an important role in evaluating a range of hepatic diseases, such as hepatitis, hepatic fibrosis, HCC, vascular invasion of liver cancer, and even HE. With the rapid development of computer technology and AI, radiomics and deep learning have become hot topics in the field of medical imaging. Compared with traditional AI, deep learning is a more advanced and intelligent learning algorithm, which was based on a neural network structure inspired by the human brain[22,23]. Radiomics has also been developed recently. It can adopt a variety of methods to extract numerous quantitative features from ultrasound, computed tomography (CT), and magnetic resonance imaging (MRI) images, then select the quantitative features related to the task, finally providing clinicians with a model based on radiomics to evaluate diagnostic and prognostic information[24,25].

### **Predicting clinical severity in alcohol-associated hepatitis patients**

Tana *et al*[26] included 34 patients with alcohol-associated hepatitis (AAH) and 35 control subjects in their study to extract texture features from computed tomography images based on random forest and deep learning convolutional neural network algorithms, which evaluated the diagnostic value of CT texture analysis for clinical severity (most notably aspartate aminotransferase) in AAH patients. Recursive feature elimination using random forest identified 23 top features for AAH categorizing, and the accuracy of deep learning for diagnosing AAH was 70% in the validation set.

### **Diagnosing or grading liver fibrosis**

According to the METAVIR scoring system[27], hepatic fibrosis can be divided into five categories: F0, no fibrosis; F1, portal fibrosis without septa; F2, portal fibrosis and few septa; F3, numerous septa without cirrhosis; F4, cirrhosis. Significant fibrosis is defined as  $\geq$  F2. Based on radiomics or deep learning algorithms, multifarious imaging modalities have been applied to diagnose or stage liver fibrosis, such as ultrasound, contrast or non-contrast CT, CT texture, MRI, or gadoteric acid-enhanced hepatobiliary phase MR.

A study including 144 HBV infected patients, evaluated the performance of multiparametric ultrasomics for the diagnosis of significant hepatic fibrosis[9]. Conventional ultrasomics, original radiofrequency, and contrast-enhanced micro-flow features comprise the multiparametric ultrasomics for clinicians to diagnose diseases and monitor treatment regimens. Multiparametric ultrasomics used Adaboost, random forest, and SVM algorithms for predicting significant liver fibrosis, with results summarized in [Table 2](#). With 466 patients (401 with chronic hepatitis B, 65 without fibrosis) undergoing partial hepatectomy used as the data of the training group and test group of transfer learning (TL) radiomics, Xue *et al*[28] discussed the diagnostic value of transfer learning radiomics based on multimodal ultrasound in the grading of liver fibrosis. As the name suggests, TL moves a network trained on a large data set on to other related tasks, thus avoiding the over fitting problem caused by insufficient training data in conventional deep learning. Results showed that the area under the curve (AUC) of TL was statistically higher than that of non-TL, and the AUC of multimodal ultrasound imaging was larger than that of single modality ultrasound imaging. Hence, multimodal ultrasound imaging based on TL could usefully be applied to the staging of liver fibrosis.

**Table 2** Hepatitis or hepatitis associated lesion detection based on radiology

No.	Task	Algorithms (model)	Sample size (type)	Evaluation index	Ref.
1	Predicting clinical severity in AAH patients	Random forest; Convolutional neural network	69 cases (CT texture features)	Accuracy: 82.4% of RFE-RF in the test set; Accuracy: 70% of CNN in the test set	[26]
2	Assessing significant liver fibrosis by multiparametric ultrasonics data	Adaboost; Random forest; SVM (multiparametric ultrasonics)	144 HBV infected patients (multiparametric ultrasonics)	AUROC: 0.85 ± 0.01 of Adaboost, random forest, SVM in multiparametric ultrasonics including conventional ultrasonics, ORF and CEMF	[9]
3	Grading liver fibrosis	Inception-V3 network (transfer learning)	466 patients (multimodal ultrasound)	AUCs of TL in GM + EM reached 0.950, 0.932, and 0.930, respectively, for grading S4, ≥ S3, and ≥ S2an	[28]
4	Predicting cirrhosis	LASSO (radiomics nomogram)	144 cases of HBV patients (CT features and clinical factors)	AUROC: 0.915 in the training cohort, 0.872 in the validation cohort, overall correctly classified rate of 82.0%	[29]
5	Differentiating hepatic fibrosis' grade	RFC (CTTA-based models); SVM (CTTA-based models)	30 fibrosis patients (CT texture features)	Train AUC 0.95 in RFC (model 1); Test AUC 0.90 in RFC (model 1); Train AUC 0.88 in SVM (model 2); Test AUC 0.76 in SVM (model 2)	[30]
6	Assessing liver fibrosis severity	A prototype convolutional neural network	558 cases (CT images)	AUCs were 0.82, 0.85, and 0.88 of Vol <sub>L</sub> /Vol <sub>S</sub> in diagnosing advanced fibrosis, cirrhosis, and decompensated cirrhosis in the whole study population	[31]
7	Staging liver fibrosis	Convolutional neural network	634 fibrosis patients (MR images and MR/virus)	AUCs were 0.84, 0.84, and 0.85 of the model full for diagnosing F4, ≥ F3, and ≥ F2 in the test set, respectively	[34]
8	Assessing liver fibrosis in chronic hepatitis B	Convolution neural network (DLRE)	398 HBV patients (shear wave elastography)	AUCs of DLRE 1.00, 0.99, and 0.99 for classifying F4, ≥ F3, and ≥ F2 in the training set and 0.97, 0.98, and 0.85 in the validation set	[35]
9	Diagnosing FNH from HCC in the non-cirrhotic liver	LASSO (radiomics nomogram)	156 patients (CT images and clinical factors)	Accuracy: 92.4% in the training set, 89.2% in the validation set	[38]
10	Diagnosing HCC	LASSO (radiomics signature)	211 patients (MR images)	AUROC: 0.861 in the training set, 0.810 in the validation set	[39]
11	Preoperative prediction of HCC grade	LASSO (combined model with clinical factors and radiomics signature)	170 HCC patients (MR images and clinical factors)	AUROC: 0.742, 0.786, and 0.800 based on T1WI images, T2WI images, and combined T1WI and T2WI images in the combined model	[41]
12	Predicting MVI risk in HBV-related HCC preoperatively	LASSO (radiomics nomogram)	304 HCC patients (CT images and AFP)	AUROC: 0.846 in the training set, 0.844 in the validation set	[43]
13	Preoperative prediction of MVI in HCC patients	LASSO (combined model)	157 HCC patients (CT images and clinical factors)	AUROC: 0.835 in the training dataset, 0.801 in the validation dataset	[44]
14	Predicting risk of HE complicated by hepatitis B related cirrhosis	LASSO (integrated model of radiomics and clinical features)	304 cirrhosis patients (CT images and clinical factors)	Accuracy: 0.93 in the training cohort, 0.83 in the testing cohort	[45]
15	Predicting liver failure in cirrhotic patients with HCC after major hepatectomy	LASSO (integrated radiomics-based mode)	101 HCC patients (MR images and clinical factors)	Accuracy: 0.802 in radiomics-based model	[47]

AAH: Alcohol-associated hepatitis; CT: Computed tomography; RFE-RF: Recursive feature elimination using random forest; CNN: Convolutional neural network; SVM: Supporter vector machine; HBV: Hepatitis B virus; AUROC: Area under the receiver operating curve; ORF: Original radiofrequency; CEMF: Contrast-enhanced micro-flow; AUC: Area under curve; TL: Transfer learning; GM: Gray scale modality; EM: Elastogram modality; LASSO: Least absolute shrinkage and selection operator; RFC: Random forest classifier; CTTA: Computed tomography texture analysis; Vol<sub>L</sub>: Liver volume; Vol<sub>S</sub>: Spleen volume; MR: Magnetic resonance; DLRE: Deep learning radiomics of shear wave elastography; FNH: Focal nodular hyperplasia; HCC: Hepatocellular carcinoma; MVI: Microvascular invasion; AFP: Alpha-fetoprotein; HE: Hepatic encephalopathy.

In another study, Wang *et al*[29] included 144 HBV patients with hepatic fibrosis

confirmed by liver biopsy who underwent unenhanced CT examinations in their study and successfully extracted 25 cirrhosis-related CT features to construct a radiomics signature using the SVM algorithm. In addition to the CT features that were closely related to liver cirrhosis, the specific clinical factors (alanine transaminase, aspartate aminotransferase, globulin, and international normalized ratio) were also closely related to liver cirrhosis. Combining the radiomics signature and clinical factors, a radiomics-based nomogram was established, and the results demonstrated that the area under the receiver operating curve (AUROC) of the radiomics nomogram was 0.915 and 0.872 in the training and validation cohorts, respectively. CT texture analysis (CTTA) revealed the biological and pathological features of diverse liver diseases by analyzing the characteristics and distribution of pixels in medical images, and extracted texture features that were difficult to recognize by the naked eye. To explore the diagnostic value of CTTA in low- and high-grade hepatic fibrosis, Budai *et al*[30] included 30 patients with liver fibrosis in the study. They extracted 354 CT texture features and constructed a CTTA-based model using a random forest classifier (RFC) algorithm and SVM algorithm, respectively. The AUROC of the CTTA-based model based on the RFC algorithm in predicting fibrosis grade was 0.90 in both the first and second analyses. The AUC of the CTTA-based model using the SVM algorithm in predicting liver fibrosis in analysis I was 0.76, and 0.91 in analysis II that was the highest prediction rate. Son *et al*[31] also evaluated liver fibrosis severity using splenic volume (measured on portal venous phase CT images). They proposed a convolution neural network (CNN) based on a three-dimensional U-net, with 513 chronic liver disease patients and 45 healthy liver subjects taken as modeled data, dividing the liver and spleen into many segments. By using the calculus method, the volume of hepatic and splenic segments in each thin slice was first calculated, then the volume of the liver and spleen in each thin slice was calculated, and finally, the volume of the liver and spleen amounted to the volume of the liver and spleen in each thin slice multiplied by the thickness of each thin slice. Then, they evaluated the correlation between liver and spleen volume indexes [ $Vol_s$  (spleen volume),  $Vol_l$  (liver volume), and  $Vol_s/Vol_l$ ] and liver fibrosis severity and their diagnostic value in liver fibrosis severity. The results demonstrated that the AUCs were 0.82, 0.85, and 0.88 of  $Vol_l/Vol_s$  for the diagnosis of advanced fibrosis, cirrhosis, and decompensated cirrhosis in the entire study population, which outperformed the  $Vol_l$ .

A variety of methods have been used to detect the stage of liver fibrosis, such as serological markers and elasticity scores based on ultrasound[32,33]. Yasaka *et al*[34] specifically included 534 patients with hepatic fibrosis into training datasets and 100 fibrosis patients into test sets, analyzing the diagnostic value of deep CNN using gadoxetic acid-enhanced hepatobiliary phase MR images and MR/virus model for liver fibrosis. The results showed that AUCs were 0.84, 0.84, and 0.85 of the model full (combined MR images and MR/virus model) for diagnosing F4,  $\geq$  F3, and  $\geq$  F2 in test sets, respectively, while 0.81, 0.84, and 0.83 of MR/virus model for diagnosing F4,  $\geq$  F3, and  $\geq$  F2 in test sets.

Previous studies have been limited to single-center studies to explore the diagnostic value of ultrasound, CT, or MRI images-based radiomics or deep learning model for liver fibrosis. Wang *et al*[35] subsequently carried out a prospective multicenter study based on deep learning radiomics of shear wave elastography (DLRE) to assess the diagnostic performance for evaluating liver fibrosis in chronic hepatitis B, and compare it with 2D-SWE (shear wave elastography) and serological biomarkers [APRI and fibrosis index based on four factors (FIB-4)]. A total of 398 patients from 12 hospitals in China with 1990 2D-SWE images were included in the study, and a DLRE model was established using the CNN algorithm. The results showed that the AUCs of DLRE were 0.97, 0.98, 0.85 for classifying F4,  $\geq$  F3, and  $\geq$  F2 in the validation set, which statistically outperformed 2D-SWE and serological biomarkers (APRI and FIB-4) except 2D-SWE in  $\geq$  F2. Simplified structural flowchart of convolutional neural network architecture for staging liver fibrosis can be seen in Figure 1.

### Diagnosing HCC

Typical focal nodular hyperplasia (FNH) has central cicatricial foci, which is enhanced in the arterial phase (AP), and the enhancement degree gradually decreases to low density in the portal venous phase (PVP). Atypical FNH has no central cicatricial foci and shows low perfusion, even hemorrhage, necrosis, and calcification on enhanced CT, which makes it difficult to differentiate atypical FNH from HCC[36,37]. Hence, Nie *et al*[38] aimed to establish a radiomics nomogram model based on CT for differentiating FNH from HCC. A total of 156 patients with FNH and HCC were divided into a training group and test group of the above-mentioned radiomics nomogram model. Initially, 4227 radiomics features were extracted from the regions of interest (ROIs) on

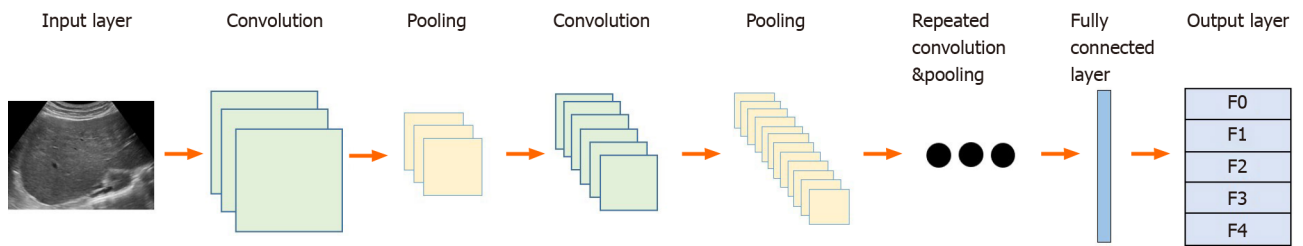


**Figure 1 Simplified structural flowchart of convolutional neural network architecture for staging liver fibrosis.** After repeatedly convoluting and pooling the input layer images, the extracted high-dimensional manageable features are fed into the fully connected layer and the classification task is performed by expressing the class probabilities through the output layer.

hepatic CT scan. After selection for inter- and intra-class correlation coefficients (ICCs)  $> 0.75$  and statistical difference between the two groups, 764 radiomics features were entered into least absolute shrinkage and selection operator (LASSO) regression, and finally, ten features were used for the construction of a radiomics signature. After multivariate logistic regression calculation, old age, HBV infection, and early enhancement (with a washout pattern) were used to establish the clinical factors model. Three models were then established: Radiomics signature model, clinical factors model, and radiomics nomogram model (clinical factors and radiomics signature combined). The predictive performance of the radiomics nomogram model was superior to those of the other constructed models. The accuracy of the radiomics nomogram model for diagnosing HCC was 92.4% and 89.2% in the training and validation datasets, respectively.

To confirm the value of the AI model for predicting HCC, Jiang *et al*[39] implemented a prospective study to compare the diagnostic differences of the 2018 European Association for the Study of the Liver (EASL) criteria, Liver Imaging Reporting and Data System (LI-RADS) criteria, and a radiomics signature model for diagnosing HCC. They included 211 patients with surgically confirmed focal liver lesions (165 HCC patients, 30 non-HCC malignancies patients, and 16 non-HCC benign lesions patients) who were randomly divided into a training cohort ( $n = 133$ ) and a validation cohort ( $n = 78$ ). The results demonstrated that the AUROCs of HCC risk in all nodules calculated by EASL v2018 criteria, LR5/LR5V in LI-RADS v2018 criteria, and radiomics signature model were 0.811, 0.841, and 0.810, respectively. The benignity and malignancy of liver tumors are usually based on Edmondson grade. Generally speaking, low-grade liver tumors conform to Edmondson I/II, while high-grade liver tumors conform to Edmondson III/IV[40]. Wu *et al*[41] included 125 HCC patients in the training group and 45 HCC patients in the validation group to predict the grade of HCC patients based on unenhanced MRI radiomics. The MRI image was uploaded to ITK-SNAP software, and the ROI was depicted along the edge of the tumor on each T1WI and T2WI segment with radiomics features extracted from ROI. A total of 656 radiomics features were extracted. After LASSO regression selection, 14, 18, and 20 features were selected based on T1WI, T2WI, and combined T1WI and T2WI, respectively. Finally, the combined model was established with results summarized in Table 2.

### Predicting microvascular invasion of HCC

The occurrence of microvascular invasion (MVI) often reduces the 5-year survival rate of HCC patients, which is closely related to the poor prognosis of HCC patients[42]. Peng *et al*[43] randomly assigned 304 cases of eligible HCC patients to the training group and validation group. IBEX software was used to extract radiomics features from the ROI of enhanced CT images in each of the HCC patients. In this study, 980 candidate radiomics features were generated from each patient, and after screening by LASSO with  $\lambda$  chosen smallest cross-validation error, eight radiomics features were selected to establish the radiomics signature. Radiomics signature, together with radiologic features (non-smooth tumor margin, internal arteries, and hypoattenuating halos) and alpha-fetoprotein  $> 20$  ng/mL, was used to construct the radiomics nomogram, whose AUROC values for predicting MVI status were 0.846 and 0.844 in the training and validation sets, respectively. Ma *et al*[44] also discussed the value of preoperative radiomics nomogram for diagnosing MVI in HCC patients based on enhanced CT; 110 HCC patients were randomly assigned to the training cohort (MVI+ group 37 cases, MVI-group 73 cases), and 47 HCC patients to the validation cohort (MVI+ group 18 cases, MVI-group 29 cases). The ROI was drawn by an experienced

radiologist using ITK-SNAP software in AP, PVP, and delayed phase (DP) images on CT along the visible borders of the lesion. Initially, in the AP, PVP, and DP images, 647 radiomics features were extracted. After screening by ICC and concordance correlation coefficient  $\geq 0.75$  and LASSO method, finally, five AP features, seven PVP features, and nine DP features were selected. In predicting HCC invasion of MVI, PVP and radiomics signature outperformed AP and DP, hence, the PVP radiomics signature with the effective clinical factors constituted the combined model, whose AUCs were 0.835 and 0.801 in the training and validation groups, respectively for diagnosing MVI status in HCC.

### **Predicting HE secondary to hepatitis B related cirrhosis**

Decompensated liver cirrhosis is often accompanied by multiple complications, of which HE is the most serious complication. Therefore, it is worthwhile to try to predict hepatic fibrosis patients who are susceptible to HE to provide early prevention and treatment[45]. A total of 304 cases of first-diagnosed hepatitis B-related cirrhosis were included in their study, 212 cases in the training group (HE = 38, non-HE = 174) and 92 cases in the validation group (HE = 21, non-HE = 71). Initially, 356 radiomics features were picked from the ROI of a patient's liver enhanced CT. After three times selection, 19 radiomics features were applied to construct a radiomics model. Three clinical factors related to HE, including serum albumin, ascites, and collateral circulation, were used to establish a clinical factor model. The results showed that, in the training and validation cohorts, the model combining radiomics and clinical features had an accuracy rate of 0.93 and 0.83 in predicting the risk of HE complicated by hepatitis B cirrhosis, respectively, while the corresponding values were 0.89 and 0.84 for radiomics model, and 0.83 and 0.77 for the clinical model.

### **Predicting liver failure in cirrhotic patients with HCC after major hepatectomy**

Postoperative hepatic failure is the most serious complication in HCC patients after hepatectomy, which not only prolongs the hospitalization time of patients but also increases the mortality of patients[46]. Zhu *et al*[47] included 101 eligible HCC patients who had a major liver resection, to use preoperative gadoteric acid-enhanced MRI for predicting liver failure based on the radiomics model. Removing the necessary structures, on the hepatobiliary phase image of the above-mentioned patient, experienced radiologists drew ROIs of the liver along the edge of the whole hepatic parenchyma. Through screening for ICC  $> 0.75$  and LASSO regression, five features were employed to establish a radiomics signature. Then, the radiomics signature and ICG-R15 (a variable in the clinical factors model) were incorporated to establish a radiomics-based model. The results showed that the accuracy of the radiomics-based model in predicting postoperative liver failure was 0.802.

---

## **CONCLUSION**

AI can mine data from patients' medical records, the Centers for Disease Control and Prevention in countries or regions, and serological markers. Raman spectroscopy can predict the incidence of hepatitis, classify the different stages of hepatitis, diagnose or screen hepatitis, forecast the progression of hepatitis, and predict response to antiviral drugs in CHC patients with a high level of diagnostic performance. AI, especially deep learning or radiomics, can predict hepatitis, predict liver fibrosis and its grade, differentiate HCC from the benign liver tumor, predict the risk of vascular invasion of HCC, predict the risk of HE complicated by hepatitis B related cirrhosis, and predict the risk of liver failure after hepatectomy in HCC patients, with good levels of accuracy.

### **Limitations and future perspectives**

At present, all reviewed studies using AI are mostly single-center research, and the amount of data in the training sets may be insufficient. In the future, people should build an internet database or hospital, and disease-related information from various countries or regions could be uploaded to the internet database or hospital so that AI researchers can obtain more disease-related information with different demographics, geographic areas, *etc.*, to carry out multicenter research, and establish a more robust and inclusive AI model for clinical use.

## REFERENCES

- 1 **Angermueller C**, Pärnamaa T, Parts L, Stegle O. Deep learning for computational biology. *Mol Syst Biol* 2016; **12**: 878 [PMID: [27474269](#) DOI: [10.15252/msb.20156651](#)]
- 2 **Zhou LQ**, Wang JY, Yu SY, Wu GG, Wei Q, Deng YB, Wu XL, Cui XW, Dietrich CF. Artificial intelligence in medical imaging of the liver. *World J Gastroenterol* 2019; **25**: 672-682 [PMID: [30783371](#) DOI: [10.3748/wjg.v25.i6.672](#)]
- 3 **Chan HP**, Samala RK, Hadjiiski LM, Zhou C. Deep Learning in Medical Image Analysis. *Adv Exp Med Biol* 2020; **1213**: 3-21 [PMID: [32030660](#) DOI: [10.1007/978-3-030-33128-3\\_1](#)]
- 4 **Gore JC**. Artificial intelligence in medical imaging. *Magn Reson Imaging* 2020; **68**: A1-A4 [PMID: [31857130](#) DOI: [10.1016/j.mri.2019.12.006](#)]
- 5 **Liang X**, Yu J, Liao J, Chen Z. Convolutional Neural Network for Breast and Thyroid Nodules Diagnosis in Ultrasound Imaging. *Biomed Res Int* 2020; **2020**: 1763803 [PMID: [32420322](#) DOI: [10.1155/2020/1763803](#)]
- 6 **Wang F**, Liu X, Yuan N, Qian B, Ruan L, Yin C, Jin C. Study on automatic detection and classification of breast nodule using deep convolutional neural network system. *J Thorac Dis* 2020; **12**: 4690-4701 [PMID: [33145042](#) DOI: [10.21037/jtd-19-3013](#)]
- 7 **Dong F**, She R, Cui C, Shi S, Hu X, Zeng J, Wu H, Xu J, Zhang Y. One step further into the blackbox: a pilot study of how to build more confidence around an AI-based decision system of breast nodule assessment in 2D ultrasound. *Eur Radiol* 2021; **31**: 4991-5000 [PMID: [33404698](#) DOI: [10.1007/s00330-020-07561-7](#)]
- 8 **Khan S**, Ullah R, Khan A, Ashraf R, Ali H, Bilal M, Saleem M. Analysis of hepatitis B virus infection in blood sera using Raman spectroscopy and machine learning. *Photodiagnosis Photodyn Ther* 2018; **23**: 89-93 [PMID: [29787817](#) DOI: [10.1016/j.pdpdt.2018.05.010](#)]
- 9 **Li W**, Huang Y, Zhuang BW, Liu GJ, Hu HT, Li X, Liang JY, Wang Z, Huang XW, Zhang CQ, Ruan SM, Xie XY, Kuang M, Lu MD, Chen LD, Wang W. Multiparametric ultrasomics of significant liver fibrosis: A machine learning-based analysis. *Eur Radiol* 2019; **29**: 1496-1506 [PMID: [30178143](#) DOI: [10.1007/s00330-018-5680-z](#)]
- 10 **Zhen S**, Cai X. Letter to the Editor: Predicting Survival After Hepatocellular Carcinoma Resection Using Deep-Learning on Histological Slides. *Hepatology* 2021; **73**: 2077-2078 [PMID: [32894573](#) DOI: [10.1002/hep.31543](#)]
- 11 **Lavanchy D**. Hepatitis B virus epidemiology, disease burden, treatment, and current and emerging prevention and control measures. *J Viral Hepat* 2004; **11**: 97-107 [PMID: [14996343](#) DOI: [10.1046/j.1365-2893.2003.00487.x](#)]
- 12 **Guan P**, Huang DS, Zhou BS. Forecasting model for the incidence of hepatitis A based on artificial neural network. *World J Gastroenterol* 2004; **10**: 3579-3582 [PMID: [15534910](#) DOI: [10.3748/wjg.v10.i24.3579](#)]
- 13 **Zheng Y**, Zhang L, Zhu X, Guo G. A comparative study of two methods to predict the incidence of hepatitis B in Guangxi, China. *PLoS One* 2020; **15**: e0234660 [PMID: [32579598](#) DOI: [10.1371/journal.pone.0234660](#)]
- 14 **Gan R**, Chen X, Yan Y, Huang D. Application of a hybrid method combining grey model and back propagation artificial neural networks to forecast hepatitis B in china. *Comput Math Methods Med* 2015; **2015**: 328273 [PMID: [25815044](#) DOI: [10.1155/2015/328273](#)]
- 15 **Guo Y**, Feng Y, Qu F, Zhang L, Yan B, Lv J. Prediction of hepatitis E using machine learning models. *PLoS One* 2020; **15**: e0237750 [PMID: [32941452](#) DOI: [10.1371/journal.pone.0237750](#)]
- 16 **Ahmad G**, Khan MA, Abbas S, Athar A, Khan BS, Aslam MS. Automated Diagnosis of Hepatitis B Using Multilayer Mamdani Fuzzy Inference System. *J Healthc Eng* 2019; **2019**: 6361318 [PMID: [30867895](#) DOI: [10.1155/2019/6361318](#)]
- 17 **Wang X**, Tian S, Yu L, Lv X, Zhang Z. Rapid screening of hepatitis B using Raman spectroscopy and long short-term memory neural network. *Lasers Med Sci* 2020; **35**: 1791-1799 [PMID: [32285292](#) DOI: [10.1007/s10103-020-03003-4](#)]
- 18 **Yehia BR**, Schranz AJ, Umscheid CA, Lo Re V 3rd. The treatment cascade for chronic hepatitis C virus infection in the United States: a systematic review and meta-analysis. *PLoS One* 2014; **9**: e101554 [PMID: [24988388](#) DOI: [10.1371/journal.pone.0101554](#)]
- 19 **Doyle OM**, Leavitt N, Rigg JA. Finding undiagnosed patients with hepatitis C infection: an application of artificial intelligence to patient claims data. *Sci Rep* 2020; **10**: 10521 [PMID: [32601354](#) DOI: [10.1038/s41598-020-67013-6](#)]
- 20 **Konerman MA**, Beste LA, Van T, Liu B, Zhang X, Zhu J, Saini SD, Su GL, Nallamothu BK, Ioannou GN, Waljee AK. Machine learning models to predict disease progression among veterans with hepatitis C virus. *PLoS One* 2019; **14**: e0208141 [PMID: [30608929](#) DOI: [10.1371/journal.pone.0208141](#)]
- 21 **Maiellaro PA**, Cozzolongo R, Marino P. Artificial neural networks for the prediction of response to interferon plus ribavirin treatment in patients with chronic hepatitis C. *Curr Pharm Des* 2004; **10**: 2101-2109 [PMID: [15279549](#) DOI: [10.2174/1381612043384240](#)]
- 22 **Chartrand G**, Cheng PM, Vorontsov E, Drozdal M, Turcotte S, Pal CJ, Kadoury S, Tang A. Deep Learning: A Primer for Radiologists. *Radiographics* 2017; **37**: 2113-2131 [PMID: [29131760](#) DOI: [10.1148/rg.2017170077](#)]
- 23 **Lee JG**, Jun S, Cho YW, Lee H, Kim GB, Seo JB, Kim N. Deep Learning in Medical Imaging: General Overview. *Korean J Radiol* 2017; **18**: 570-584 [PMID: [28670152](#) DOI: [10.3348/kjr.2016.18.5.570](#)]

- 10.3348/kjr.2017.18.4.570]
- 24 **Gillies RJ**, Kinahan PE, Hricak H. Radiomics: Images Are More than Pictures, They Are Data. *Radiology* 2016; **278**: 563-577 [PMID: 26579733 DOI: 10.1148/radiol.2015151169]
  - 25 **Lee G**, Lee HY, Park H, Schiebler ML, van Beek EJR, Ohno Y, Seo JB, Leung A. Radiomics and its emerging role in lung cancer research, imaging biomarkers and clinical management: State of the art. *Eur J Radiol* 2017; **86**: 297-307 [PMID: 27638103 DOI: 10.1016/j.ejrad.2016.09.005]
  - 26 **Tana MM**, McCoy D, Lee B, Patel R, Lin J, Ohliger MA. Texture features from computed tomography correlate with markers of severity in acute alcohol-associated hepatitis. *Sci Rep* 2020; **10**: 17980 [PMID: 33087739 DOI: 10.1038/s41598-020-74599-4]
  - 27 **Husain A**, Chihwane A, Kirnake V. Non-invasive assessment of liver fibrosis in alcoholic liver disease. *Clin Exp Hepatol* 2020; **6**: 125-130 [PMID: 32728629 DOI: 10.5114/ceh.2020.95739]
  - 28 **Xue LY**, Jiang ZY, Fu TT, Wang QM, Zhu YL, Dai M, Wang WP, Yu JH, Ding H. Transfer learning radiomics based on multimodal ultrasound imaging for staging liver fibrosis. *Eur Radiol* 2020; **30**: 2973-2983 [PMID: 31965257 DOI: 10.1007/s00330-019-06595-w]
  - 29 **Wang JC**, Fu R, Tao XW, Mao YF, Wang F, Zhang ZC, Yu WW, Chen J, He J, Sun BC. A radiomics-based model on non-contrast CT for predicting cirrhosis: make the most of image data. *Biomark Res* 2020; **8**: 47 [PMID: 32963787 DOI: 10.1186/s40364-020-00219-y]
  - 30 **Budai BK**, Tóth A, Borsos P, Frank VG, Shariati S, Fejér B, Folhoffer A, Szalay F, Bérczi V, Kaposi PN. Three-dimensional CT texture analysis of anatomic liver segments can differentiate between low-grade and high-grade fibrosis. *BMC Med Imaging* 2020; **20**: 108 [PMID: 32957949 DOI: 10.1186/s12880-020-00508-w]
  - 31 **Son JH**, Lee SS, Lee Y, Kang BK, Sung YS, Jo S, Yu E. Assessment of liver fibrosis severity using computed tomography-based liver and spleen volumetric indices in patients with chronic liver disease. *Eur Radiol* 2020; **30**: 3486-3496 [PMID: 32055946 DOI: 10.1007/s00330-020-06665-4]
  - 32 **Talwalkar JA**, Kurtz DM, Schoenleber SJ, West CP, Montori VM. Ultrasound-based transient elastography for the detection of hepatic fibrosis: systematic review and meta-analysis. *Clin Gastroenterol Hepatol* 2007; **5**: 1214-1220 [PMID: 17916549 DOI: 10.1016/j.cgh.2007.07.020]
  - 33 **Friedrich-Rust M**, Ong MF, Martens S, Sarrazin C, Bojunga J, Zeuzem S, Herrmann E. Performance of transient elastography for the staging of liver fibrosis: a meta-analysis. *Gastroenterology* 2008; **134**: 960-974 [PMID: 18395077 DOI: 10.1053/j.gastro.2008.01.034]
  - 34 **Yasaka K**, Akai H, Kunimatsu A, Abe O, Kiryu S. Liver Fibrosis: Deep Convolutional Neural Network for Staging by Using Gadoteric Acid-enhanced Hepatobiliary Phase MR Images. *Radiology* 2018; **287**: 146-155 [PMID: 29239710 DOI: 10.1148/radiol.2017171928]
  - 35 **Wang K**, Lu X, Zhou H, Gao Y, Zheng J, Tong M, Wu C, Liu C, Huang L, Jiang T, Meng F, Lu Y, Ai H, Xie XY, Yin LP, Liang P, Tian J, Zheng R. Deep learning Radiomics of shear wave elastography significantly improved diagnostic performance for assessing liver fibrosis in chronic hepatitis B: a prospective multicentre study. *Gut* 2019; **68**: 729-741 [PMID: 29730602 DOI: 10.1136/gutjnl-2018-316204]
  - 36 **Yu Y**, Lin X, Chen K, Chai W, Hu S, Tang R, Zhang J, Cao L, Yan F. Hepatocellular carcinoma and focal nodular hyperplasia of the liver: differentiation with CT spectral imaging. *Eur Radiol* 2013; **23**: 1660-1668 [PMID: 23306709 DOI: 10.1007/s00330-012-2747-0]
  - 37 **Grazioli L**, Bondioni MP, Faccioli N, Gambarini S, Tinti R, Schneider G, Kirchin M. Solid focal liver lesions: dynamic and late enhancement patterns with the dual phase contrast agent gadobenate dimeglumine. *J Gastrointest Cancer* 2010; **41**: 221-232 [PMID: 20405242 DOI: 10.1007/s12029-010-9145-0]
  - 38 **Nie P**, Yang G, Guo J, Chen J, Li X, Ji Q, Wu J, Cui J, Xu W. A CT-based radiomics nomogram for differentiation of focal nodular hyperplasia from hepatocellular carcinoma in the non-cirrhotic liver. *Cancer Imaging* 2020; **20**: 20 [PMID: 32093786 DOI: 10.1186/s40644-020-00297-z]
  - 39 **Jiang H**, Liu X, Chen J, Wei Y, Lee JM, Cao L, Wu Y, Duan T, Li X, Ma L, Song B. Man or machine? *Cancer Imaging* 2019; **19**: 84 [PMID: 31806050 DOI: 10.1186/s40644-019-0266-9]
  - 40 **Edmondson HA**, Steiner PE. Primary carcinoma of the liver: a study of 100 cases among 48,900 necropsies. *Cancer* 1954; **7**: 462-503 [PMID: 13160935 DOI: 10.1002/1097-0142(195405)7:3<462::aid-cnrcr2820070308>3.0.co;2-e]
  - 41 **Wu M**, Tan H, Gao F, Hai J, Ning P, Chen J, Zhu S, Wang M, Dou S, Shi D. Predicting the grade of hepatocellular carcinoma based on non-contrast-enhanced MRI radiomics signature. *Eur Radiol* 2019; **29**: 2802-2811 [PMID: 30406313 DOI: 10.1007/s00330-018-5787-2]
  - 42 **Bruix J**, Llovet JM. Hepatitis B virus and hepatocellular carcinoma. *J Hepatol* 2003; **39** Suppl 1: S59-S63 [PMID: 14708679 DOI: 10.1016/s0168-8278(03)00140-5]
  - 43 **Peng J**, Zhang J, Zhang Q, Xu Y, Zhou J, Liu L. A radiomics nomogram for preoperative prediction of microvascular invasion risk in hepatitis B virus-related hepatocellular carcinoma. *Diagn Interv Radiol* 2018; **24**: 121-127 [PMID: 29770763 DOI: 10.5152/dir.2018.17467]
  - 44 **Ma X**, Wei J, Gu D, Zhu Y, Feng B, Liang M, Wang S, Zhao X, Tian J. Preoperative radiomics nomogram for microvascular invasion prediction in hepatocellular carcinoma using contrast-enhanced CT. *Eur Radiol* 2019; **29**: 3595-3605 [PMID: 30770969 DOI: 10.1007/s00330-018-5985-y]
  - 45 **Cao JM**, Yang JQ, Ming ZQ, Wu JL, Yang LQ, Chen TW, Li R, Ou J, Zhang XM, Mu QW, Li HJ, Hu J. A radiomics model of liver CT to predict risk of hepatic encephalopathy secondary to hepatitis B related cirrhosis. *Eur J Radiol* 2020; **130**: 109201 [PMID: 32738462 DOI: 10.1016/j.ejrad.2020.109201]
  - 46 **Lock JF**, Reinhold T, Malinowski M, Pratschke J, Neuhaus P, Stockmann M. The costs of

- postoperative liver failure and the economic impact of liver function capacity after extended liver resection--a single-center experience. *Langenbecks Arch Surg* 2009; **394**: 1047-1056 [PMID: 19533168 DOI: 10.1007/s00423-009-0518-4]
- 47 **Zhu WS**, Shi SY, Yang ZH, Song C, Shen J. Radiomics model based on preoperative gadoxetic acid-enhanced MRI for predicting liver failure. *World J Gastroenterol* 2020; **26**: 1208-1220 [PMID: 32231424 DOI: 10.3748/wjg.v26.i11.1208]



Published by **Baishideng Publishing Group Inc**  
7041 Koll Center Parkway, Suite 160, Pleasanton, CA 94566, USA

**Telephone:** +1-925-3991568

**E-mail:** [bpgoffice@wjgnet.com](mailto:bpgoffice@wjgnet.com)

**Help Desk:** <https://www.f6publishing.com/helpdesk>

<https://www.wjgnet.com>

